MOLECULAR AND CELLULAR BIOLOGY, Dec. 2005, p. 11145–11155 Vol. 25, No. 24
0270-7306/05/$08.00+0 doi:10.1128/MCB.25.24.11145–11155.2005

Targeted Deletion of Integrin-Linked Kinase Reveals a Role in T-Cell Chemotaxis and Survival

Emerson Liu,[1]† Sumita Sinha,[1]† Christine Williams,[2] Marcoli Cyrille,[1] Eric Heller,[1] Scott B. Snapper,[3] Katia Georgopoulos,[3] Rene St-Arnaud,[4] Thomas Force,[5] Shoukat Dedhar,[6] and Robert E. Gerszten[1]*

Center for Immunology and Inflammatory Diseases & Cardiology Division, Massachusetts General Hospital, Charlestown, Massachusetts, and Harvard Medical School, Boston, Massachusetts[1]; Cutaneous Biology Research Center, Massachusetts General Hospital, Charlestown, Massachusetts, and Harvard Medical School, Boston, Massachusetts[2]; Gastrointestinal Unit, Massachusetts General Hospital, and Harvard Medical School, Boston, Massachusetts[3]; Shriners Hospital and McGill University, Montreal, Quebec, Canada[4]; Molecular Cardiology Research Institute, New England Medical Center, Tufts University School of Medicine, Boston, Massachusetts[5]; and Department of Biochemistry and Molecular Biology, University of British Columbia, and Jack Bell Cancer Centre at Vancouver General Hospital and Health Service Center, Vancouver, British Columbia, Canada[6]

Received 17 August 2005/Accepted 7 September 2005

Integrin-linked kinase (ILK) is a serine/threonine kinase that is important in cell-matrix interactions and cell signaling. To examine the role of ILK in leukocyte trafficking and survival, we generated T cell-specific ILK knockouts by breeding $ILK^{flox/flox}$ mice to transgenic mice expressing Cre recombinase under control of the Lck proximal promoter. Thymic T cells from Lck-Cre^{+}/$ILK^{flox/flox}$ mice had a marked reduction (>95%) in ILK protein levels. Thymic cellularity was comparable in 3- to 4-week-old mice, but a threefold diminution of thymic T cells became evident by 6 to 8 weeks of age in the T cell-specific ILK knockout mice due to increased cell death of double-positive (DP) T cells. Analysis of peripheral T cells by quantitative PCR and by breeding Lck-Cre^{+}/$ILK^{flox/flox}$ mice to a YFP-transgenic reporter strain demonstrated an approximate 20-fold enrichment of ILK-competent cells, suggesting these cells have a competitive advantage in trafficking to and/or survival in peripheral lymphatic organs. We explored mechanisms related to altered cell trafficking and survival that might explain the decreases in thymic cellularity and enrichment for ILK-competent cells in the spleen and lymph nodes. We observed a >50% reduction in chemotaxis of ILK-deficient T cells to the chemokines CXCL12 (stromal cell-derived factor [SDF]-1α) and CCL19 (macrophage inflammatory protein [MIP]-3β), as well as enhanced apoptosis of ILK-deficient cells upon stress. Signaling studies in ILK-deficient T cells demonstrated diminished phosphorylation of Akt on the activating phosphorylation site, Ser 473, and a concordant decrease in Akt kinase activity following stimulation with the chemokine SDF-1. Rac1 activation was also markedly diminished in ILK-deficient T cells following chemokine stimulation. These data extend the role of ILK to immune-cell trafficking and survival via modulation of Akt- and Rac-dependent substrates, and have implications for cell recruitment in both homeostatic and pathological processes.

Chemoattractant cytokines, or chemokines, orchestrate the directional migration of leukocytes through tissues. In vitro and in vivo models suggest a functional role for chemokines in a variety of human inflammatory pathologies, including those of asthma, arthritis, and atherosclerosis (15). While several of the functionally relevant chemokine-triggered signaling pathways have been recently elucidated (4, 8, 11, 14, 22, 25), a comprehensive understanding of the mechanisms by which chemokines enhance leukocyte migration remains incomplete.

Recent data from several lines of investigation suggest an important role for integrin-linked kinase (ILK) in cell matrix interactions and cell signaling (6, 21, 26). ILK was originally identified in a yeast two-hybrid screen for proteins capable of interacting with β-integrins (10). Sequencing of ILK revealed a 59-kDa protein, serine-threonine kinase, with multiple distinct domains. The C terminus interacts with β-integrins and also contains the kinase catalytic domain. In vitro, ILK can phosphorylate synthetic peptides corresponding to β1-integrin cytoplasmic domains (10), and other substrates include Akt (26, 27) and glycogen synthase kinase 3 (GSK-3) (1). A central pleckstrin-homology domain is thought to be important for the binding of lipid second messengers. Finally, the N-terminal ankryn repeats, as well as the carboxyl terminus, may mediate integrin-cytoskeletal organization via complexes which include PINCH and the α- and β-parvin protein family, respectively (9, 18, 30).

From a functional perspective, ILK overexpression in epithelial cells disrupts cell-extracellular matrix as well as cell-cell interactions (10). Studies in transfected fibroblasts suggest a role for ILK in cell motility via its interaction with the focal adhesion protein PINCH (30). More recent studies have demonstrated robust expression of ILK in mononuclear leukocytes, which is potently activated by chemokines in a phosphoinositide 3-kinase (PI 3-K)-dependent manner. Overexpression of ILK in THP-1 monocytic cells negatively modulates adhesion to endothelial cells under flow (3).

* Corresponding author. Mailing address: Center for Immunology and Inflammatory Diseases, Massachusetts General Hospital East—8307, 149 13th Street, Charlestown, MA 02129. Phone: (617) 724-8322. Fax: (617) 726-5651. E-mail: rgerszten@partners.org.
† Contributed equally to this work.

To more definitively address the physiological role of ILK, investigators have turned to genetic models. Deletion of ILK in *Caenorhabditis elegans* leads to embryonic demise that resembles the phenotype of β-integrin knockouts (16). Similarly, complete knockout in mice confers peri-implantation lethality, as ILK is critical for the polarization of the epiblast (21). More recent studies have shown that tissue-specific deletion of ILK in chondrocytes leads to abnormalities in bone proliferation and dwarfism (6, 26), and endothelial-specific deletion of ILK inhibits vascularization and is lethal (2). For the present studies, we employed the Cre-Lox system to define the role of endogenous ILK in leukocyte biology. We used a murine system with the Lck-Cre promoter driving the expression of Cre recombinase in T cells as a representative leukocyte for investigation. Our genetic studies extend the role of ILK to immune cell trafficking and survival.

MATERIALS AND METHODS

Murine system. We employed a recently generated mouse strain carrying a LoxP-flanked (floxed) ILK gene ($ILK^{flox/flox}$), which has been previously described in detail (2, 27). To delete ILK in vivo in T cells, $ILK^{flox/flox}$ mice were bred to transgenic mice expressing Cre recombinase under the direction of the Lck proximal promoter (from Katia Georgopoulos, Massachusetts General Hospital) to generate Lck-Cre^{+}/$ILK^{flox/flox}$ mice (7, 12). Screening of tail DNA for inheritance of the floxed ILK gene was performed by PCR as previously reported (2). Inheritance of the Lck-Cre transgene was determined by PCR using the following primers: forward, 5′-CAGTCAGGAGCTTGAATCCCACGA-3′; and reverse, 5′-TAATCGCCATCTTCCAGCAG-3′. DNAs were amplified for 34 cycles (94°C for 30 s, 56°C for 45 s, and 72°C for 1 min) in a thermal cycler.

To further characterize the effects of ILK deficiency on T cells, we crossed our Lck-Cre^{+}/$ILK^{flox/flox}$ mice with Rosa-YFP reporter mice (24). Use of the transgenic reporter mouse allowed us to identify YFP^{+}, Cre-expressing T cells using flow cytometry.

Quantitative PCR. For each experiment, leukocytes were harvested in parallel from thymus and lymph nodes from the same $ILK^{flox/flox}$ mice, with or without the Lck-Cre transgene. T cells were purified using a Dynabeads Mouse pan T immunomagnetic cell isolation kit (Dynal Biotech product no. 114.03), which binds with >95% selectivity to T cells. Rosetted cells were washed three times in buffer, lysed, and utilized directly for downstream PCR analysis. Multiplexed, real-time quantitative DNA PCRs were prepared using the Quantitative PCR SuperMix-UDG system (Invitrogen) in 25-μl volumes containing 10 μM 6-carboxyfluorescein-labeled ILK primer, 10 μM JOE-labeled β-actin primer, and ROX reference dye. Primers were designed using Invitrogen's LUX Designer software online, with the ILK primer set flanking one of the LoxP sites such that only full-length floxed-ILK sequences were amplified. Reactions were run in six to nine replicates in optical 96-well strips with optical caps in an MX4000 multiplex quantitative PCR system (Stratagene). We used the recommended MX3000P optimized cycling program: 50°C, 2 min (1 cycle); 95°C, 2 min (1 cycle); 40 to 50 cycles of 54°C, 15 s; 60°C, 30 s (triplicate acquire); 72°C, 30 s; 95°C, 1 min (1 cycle). Amplification plots were analyzed using the methods of Peirson et al. (19), in which relative quantification is corrected for different amplification efficiencies of target and internal control genes. The relative abundance of intact ILK gene was calculated as the ratio of the amount of ILK gene normalized to β-actin gene in peripheral T cells from spleen or lymph node compared to that in thymic T cells.

Leukocyte isolation. Leukocytes were freshly harvested from thymus, spleen, or lymph nodes as indicated. Cell suspensions from spleen or lymph nodes were negatively enriched for T cells through magnetic bead depletion of B cells, NK cells, monocytes/macrophages, dendritic cells, granulocytes, and erythrocytes (Dynal). For in vitro proliferation assays, lymph node (LN) T cells were column purified by negative selection (Cedarlane). For studies using the YFP reporter strains, lymph node T cells were purified by staining with anti-CD3 antibody and sorting $CD3^{+}$ YFP^{+} and $CD3^{+}$ YFP^{-} populations using a Mo-Flo cell sorter (DakoCytomation).

Chemotaxis assays. For chemotaxis assays, cells were resuspended in RPMI 1640 with 0.1% bovine serum albumin (2.5×10^4 cells in 25 μl) and placed in the upper wells of a 96-transwell chemotaxis chamber (Neuro Probe, Inc.), with the lower wells containing chemokines in the same buffer, at the indicated concentrations. Following incubation at 37°C in 5% CO_2 for 90 min, the number of migrated cells in the lower chamber was manually counted using a Nikon microscope with a 10× objective.

Antibodies. Western analysis employed antibodies to ILK (Upstate Biotechnology), Cre (BioMol), phospho-Erk1/2 and total Erk1/2, and phospho-Akt (S473) and total Akt (both Cell Signaling). For fluorescence-activated cell sorter analysis, we used antibodies to CD4, CD8, TCRβ, CD25, CD44, CD45RB, immunoglobulin M, B220, Mac-1, Gr-1, Ter119, total β1-integrin (anti-CD29), and $CXCR_4$ as well as the corresponding isotype-matched controls (all from BD-Pharmingen; see flow-cytometric analysis as well). β-actin antibody was from AbCam. Western analysis employing the indicated antibody was performed as previously described in detail (3, 17).

Flow-cytometric analysis. For immunophenotyping studies, cell populations were resuspended in 100 μl of assay buffer and blocked with Fc block (Pharmingen) for 20 min at room temperature. Cells were then stained with the indicated primary conjugated antibodies, washed, and either analyzed immediately or fixed in 2% paraformaldehyde. Analysis was performed on either a Becton Dickinson FACSCalibur or FACSCanto machine and using FlowJo 6 software (Tree Star, Inc., San Carlos, CA). Purification of double-negative (DN)-thymocyte subsets was performed by staining unfractionated thymocytes with a cocktail of fluorescein isothiocyanate-labeled lineage-specific antibodies (CD4, CD8, B220, Mac-1/CD11b, GR-1/Ly6, TCRγδ, Ter119/Ly-76), APC-CD44, and PE-CD25. For analysis of cell death, cells were washed and resuspended in 100 μl binding buffer (140 mM NaCl, 10 mM HEPES/NaOH (pH 7.4), 2.5 mM $CaCl_2$), then incubated at room temperature for 15 min in the dark with 1 μl annexin V-fluorescein isothiocyanate (BD Biosciences) and 1 μl propidium iodide (BD Biosciences). After staining, the cells were diluted with an additional 400 μl of binding buffer and analyzed immediately on the flow cytometer. LN T cells were purified using antibody staining and sheep anti-rat immunoglobulin Dynabeads (Dynal Biotech Inc., Lake Success, NY) or T-cell purification columns (Cedarlane Laboratories) according to the manufacturers' protocols.

T cell proliferative responses. Flat-bottomed 96-well tissue culture plates were coated with anti-CD3ε (10 μg/ml). Unfractionated LN or purified T cells were plated in triplicate at 5×10^4 or 1×10^5 cells/well in RPMI medium supplemented with 10% fetal calf serum, 2 mM L-glutamine, 10 mM HEPES, 50 μM β-mercaptoethanol, and 100 μg/ml penicillin-streptomycin. After 48 h of culture, cells were pulsed for 12 h with [^{3}H]methyl thymidine (2 μCi/well), harvested (Harvester 96, TomTec), and counted (Betaplate Counter, Wallac).

Akt kinase assay. Akt kinase activity was assessed using a nonradioactive assay kit (Cell Signaling) according to the manufacturer's instructions, as previously reported (2). Samples were analyzed by Western blotting using an antibody specific for the sites phosphorylated by Akt on the substrate peptide (anti-phospho-GSK-3 S21/S9).

Rac kinase assay. Purified T cells were activated with the indicated chemokines at 37°C and then harvested in lysis buffer (50 mM HEPES [pH 7.5], 30 mM NaCl, 1% Igepal CA-630, 10 mM $MgCl_2$, 1 mM EDTA, 10% glycerol, 25 mM NaF, 1 mM sodium orthovanadate, and protease inhibitors) at 4°C. Whole-cell lysates were precleared and then incubated with PAK-1 PBD bound to SwellGel immobilized glutathione disks in a spin column (Pierce Biotechnology) for 60 min at 4°C with rocking. In parallel, whole-cell lysates from unstimulated cells were incubated with 100 μM of GTPγS (positive control) or GDP (negative control) for 15 min at 30°C with agitation and then processed as above. The resins were washed three times with cell lysis buffer, and GTP-bound Rac was released from beads by addition of 2× Laemmli reducing sample buffer with 2-mercaptoethanol and dithiothreitol and boiled at 100°C for 5 min. Samples were resolved by 12% sodium dodecyl sulfate-polyacrylamide gel electrophoresis for Western blotting and probed with an anti-Rac antibody (Pierce Biotechnology).

Apoptosis assays. Lymphocyte apoptosis was assessed by three independent methods: cell death detection enzyme-linked immunosorbent assay (ELISA) measuring cytoplasmic histone-associated DNA fragmentation (Roche), Western blot analysis for cleaved caspase-3 (Cell Signaling), according to the manufacturers' instructions, and flow-cytometric analysis of annexin V and propidium iodide, as detailed above (2).

Statistical analysis. Data are expressed as the means ± standard deviations or standard errors of the means, as indicated. Statistical comparison of means was performed by the two-tailed unpaired Student *t* test. The null hypothesis was rejected at a *P* value of <0.05.

RESULTS

To delete ILK in vivo in T cells, we bred $ILK^{flox/flox}$ mice to transgenic mice expressing Cre recombinase under the direction

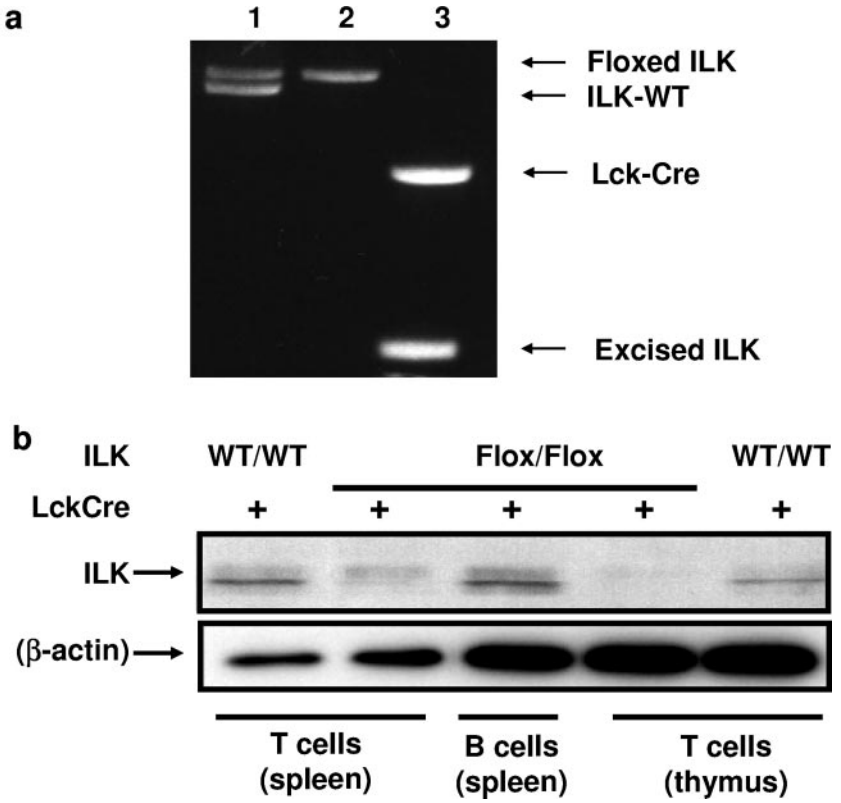

FIG. 1. T cell-specific deletion of ILK in mice. (a) $ILK^{flox/flox}$ mice were bred to transgenic mice expressing Cre recombinase under the direction of the Lck proximal promoter, and the progeny were genotyped by PCR for the inheritance of Cre recombinase and ILK using tail DNA. Representative PCR analyses of deletions in thymocytes from three mice are shown: lane 1, Cre^- $ILK^{wt/flox}$; lane 2, Cre^- $ILK^{flox/flox}$; lane 3, $Cre^+/ILK^{flox/flox}$. (b) Western blot analysis of cell lysates from Lck-$Cre^+/ILK^{flox/flox}$ mice demonstrated a marked reduction in ILK protein levels in both thymic and splenic T cells, compared to splenic B cells from the same mice, or T cells from thymus and spleen of Lck-$Cre^+/ILK^{WT/WT}$ mice (right). Densitometry confirmed a >95% reduction (not shown). Representative data from one of eight independent experiments are shown.

of the Lck proximal promoter. The resulting $Cre^+/ILK^{flox/flox}$ mice provided a well-validated system for dissecting the role of ILK in leukocyte biology through Cre-mediated deletion in developing T cells (7, 12). Screening of tail DNA for inheritance of Cre recombinase and floxed ILK alleles was performed by PCR as previously described (2). Representative data from the genotyping of mice are shown in Fig. 1a. Thymic T cells from Lck-$Cre^+/ILK^{flox/flox}$ mice had a marked reduction in ILK protein levels, as seen in Fig. 1b.

The genotypes of more than 900 offspring followed the predicted Mendelian distribution. Mice showed no gross developmental abnormalities and were fertile. As Cre driven by the Lck proximal promoter is activated early in T-cell development, we next analyzed thymuses from mice with ILK deletion versus those from littermate controls. Thymic cellularity was comparable in 3- to 4-week-old mice; however, there was a threefold reduction of thymic T cells in ILK-deficient mice by 6 to 8 weeks of age (Fig. 2a). Flow-cytometric analysis of thymocytes from 6- to 8-week-old mice revealed a diminution in both the percentages (~1.5-fold) and absolute numbers (~14-fold) of the double-positive ($CD4^+$ $CD8^+$ DP) thymic T-cell population, accompanied by a relative increase in the percentage of double-negative ($CD4^-$ $CD8^-$ DN) and single-positive ($CD4^+$ or $CD8^+$ SP) cells (Fig. 2b, top). In contrast, thymocytes from 3- to 4-week-old mice were phenotypically indistinguishable from wild-type controls (data not shown). T-cell receptor (TCR) profiles of thymocytes of the 6- to 8-week-old mice also revealed a concordant decrease in the TCR^{med} populations (Fig. 2b, middle), which normally represent DP cells, and a relative increase in TCR^{hi} single-positive (SP) cells. Staining with annexin V and propidium iodide (PI) demonstrated an approximate three- to fourfold increase in the annexin V^+/PI^+ dead cells in the ILK-deficient thymus (Fig. 2c). To rule out the possibility of an early developmental defect caused by ILK deficiency, we analyzed the DN-thymocyte precursor population in greater detail (Fig. 2d). An increase in the percentage of cells falling in the Lin^- DN gate was observed in the 6- to 8-week ILK-deficient thymus due to the depletion of the DP compartment. However, the proportion and absolute number of cells in the DN1 through DN4 stages of development, as identified by CD25 and CD44 costaining, was comparable between wild-type and ILK-deficient mice. Taken together, these results suggest that ILK deletion does not cause a thymocyte developmental defect but rather confers an increased susceptibility to cell death in the thymus that primarily affects DP T cells. Of note, no changes were noted in other thymic constituents such as TCR$\gamma\delta$ T cells (data not shown).

We conducted studies on peripheral T cells in parallel with our initial characterization of thymic T cells. While thymic T

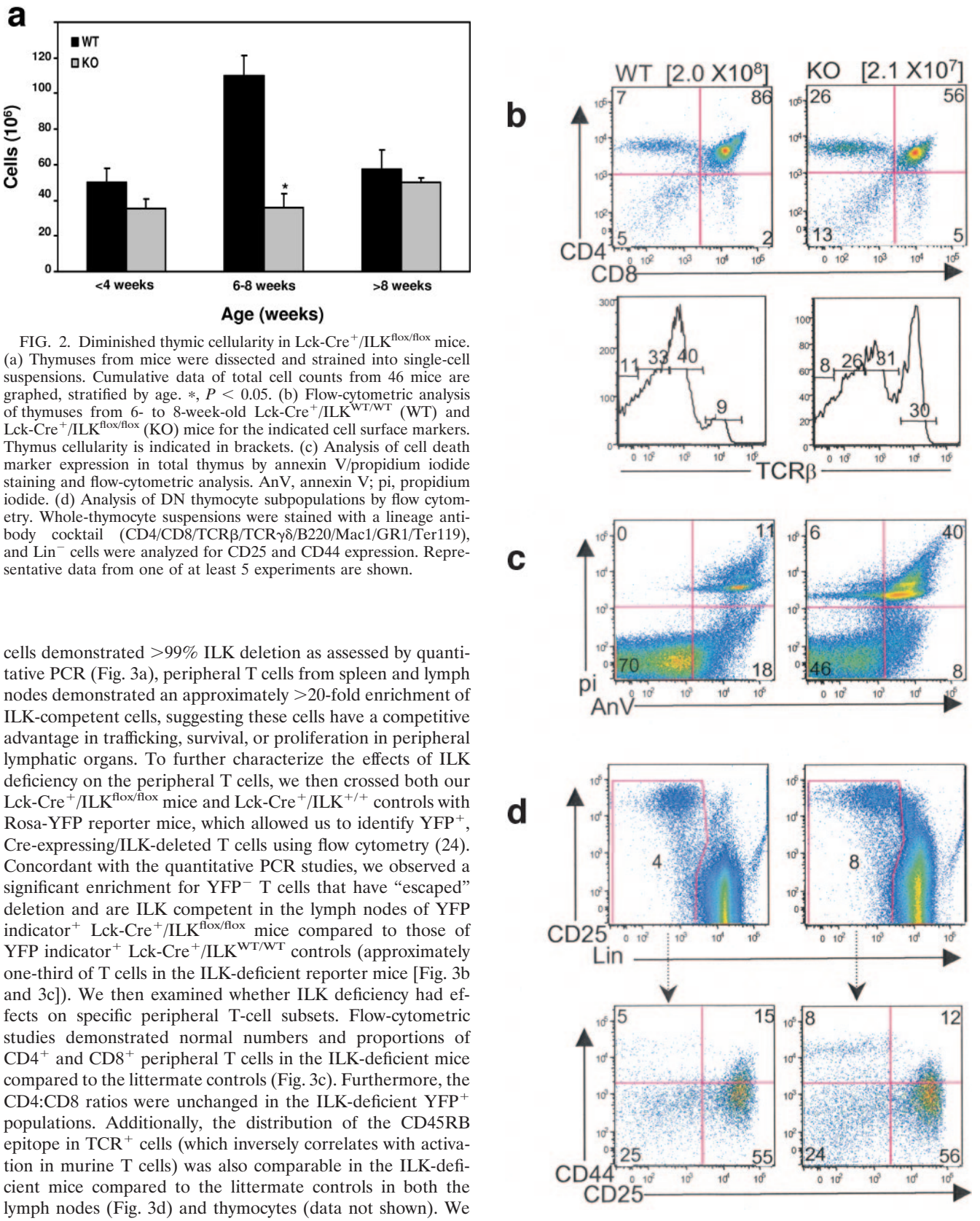

FIG. 2. Diminished thymic cellularity in Lck-Cre$^+$/ILK$^{flox/flox}$ mice. (a) Thymuses from mice were dissected and strained into single-cell suspensions. Cumulative data of total cell counts from 46 mice are graphed, stratified by age. *, $P < 0.05$. (b) Flow-cytometric analysis of thymuses from 6- to 8-week-old Lck-Cre$^+$/ILK$^{WT/WT}$ (WT) and Lck-Cre$^+$/ILK$^{flox/flox}$ (KO) mice for the indicated cell surface markers. Thymus cellularity is indicated in brackets. (c) Analysis of cell death marker expression in total thymus by annexin V/propidium iodide staining and flow-cytometric analysis. AnV, annexin V; pi, propidium iodide. (d) Analysis of DN thymocyte subpopulations by flow cytometry. Whole-thymocyte suspensions were stained with a lineage antibody cocktail (CD4/CD8/TCRβ/TCRγδ/B220/Mac1/GR1/Ter119), and Lin$^-$ cells were analyzed for CD25 and CD44 expression. Representative data from one of at least 5 experiments are shown.

cells demonstrated >99% ILK deletion as assessed by quantitative PCR (Fig. 3a), peripheral T cells from spleen and lymph nodes demonstrated an approximately >20-fold enrichment of ILK-competent cells, suggesting these cells have a competitive advantage in trafficking, survival, or proliferation in peripheral lymphatic organs. To further characterize the effects of ILK deficiency on the peripheral T cells, we then crossed both our Lck-Cre$^+$/ILK$^{flox/flox}$ mice and Lck-Cre$^+$/ILK$^{+/+}$ controls with Rosa-YFP reporter mice, which allowed us to identify YFP$^+$, Cre-expressing/ILK-deleted T cells using flow cytometry (24). Concordant with the quantitative PCR studies, we observed a significant enrichment for YFP$^-$ T cells that have "escaped" deletion and are ILK competent in the lymph nodes of YFP indicator$^+$ Lck-Cre$^+$/ILK$^{flox/flox}$ mice compared to those of YFP indicator$^+$ Lck-Cre$^+$/ILK$^{WT/WT}$ controls (approximately one-third of T cells in the ILK-deficient reporter mice [Fig. 3b and 3c]). We then examined whether ILK deficiency had effects on specific peripheral T-cell subsets. Flow-cytometric studies demonstrated normal numbers and proportions of CD4$^+$ and CD8$^+$ peripheral T cells in the ILK-deficient mice compared to the littermate controls (Fig. 3c). Furthermore, the CD4:CD8 ratios were unchanged in the ILK-deficient YFP$^+$ populations. Additionally, the distribution of the CD45RB epitope in TCR$^+$ cells (which inversely correlates with activation in murine T cells) was also comparable in the ILK-deficient mice compared to the littermate controls in both the lymph nodes (Fig. 3d) and thymocytes (data not shown). We thus observed a global enrichment for "ILK-sufficient cells" in the triple-transgenic animals, rather than subset-specific effects. Discrepancies in the number of resident T cells and the

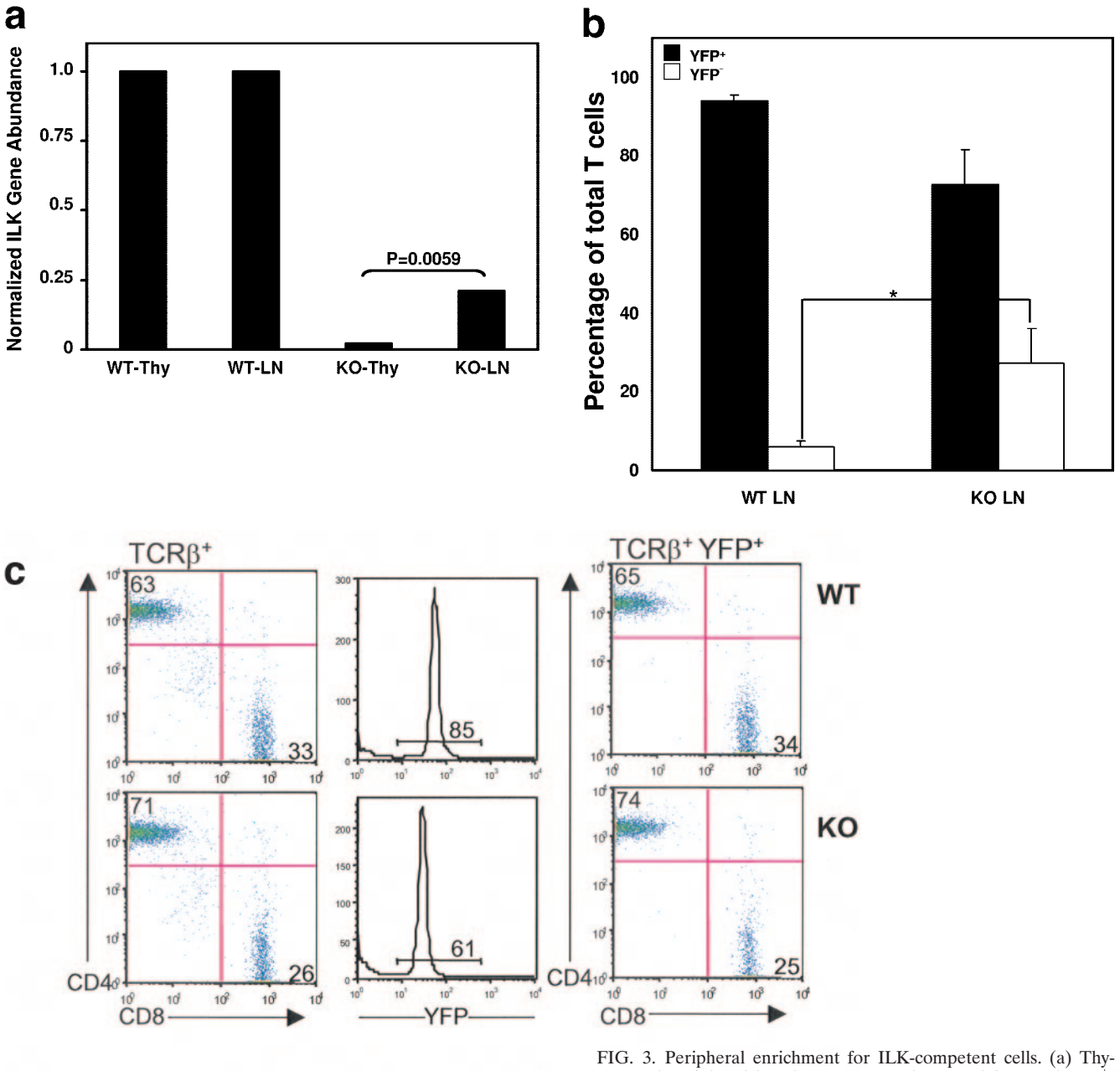

FIG. 3. Peripheral enrichment for ILK-competent cells. (a) Thymuses and peripheral lymph organs were harvested from Lck-Cre$^+$/ILK$^{flox/flox}$ and control mice, and the T cells were purified by positive selection. Real time PCR was used to determine the relative abundance of intact ILK gene in lymph node T cells compared to thymic T cells in each mouse as described in Materials and Methods. Thy, thymic. (b) Lck-Cre$^+$/ILK$^{flox/flox}$ mice and Lck-Cre$^+$/ILK$^{WT/WT}$ controls were bred into the Rosa-YFP reporter strain. Cumulative data from YFP indicator$^+$ Lck-Cre$^+$/ILK$^{flox/flox}$ mice ($n = 7$) and YFP indicator$^+$ Lck-Cre$^+$/ILK$^{WT/WT}$ mice ($n = 9$) are shown. *, $P < 0.02$. (c) Flow-cytometric analysis of CD4/CD8 ratios in TCRβ$^+$ (left) and TCRβ$^+$ YFP$^+$ (right) populations in YFP indicator$^+$ Lck-Cre$^+$/ILK$^{flox/flox}$ (KO) mice and YFP indicator$^+$ Lck-Cre$^+$/ILK$^{WT/WT}$ (WT) mice. Representative data from one of four experiments are shown. (d) Distribution of the CD45RB epitope in LN cells from Lck-Cre$^+$/ILK$^{flox/flox}$ (KO) mice and Lck-Cre$^+$/ILK$^{WT/WT}$ (WT) mice. Representative data from one of four experiments are shown.

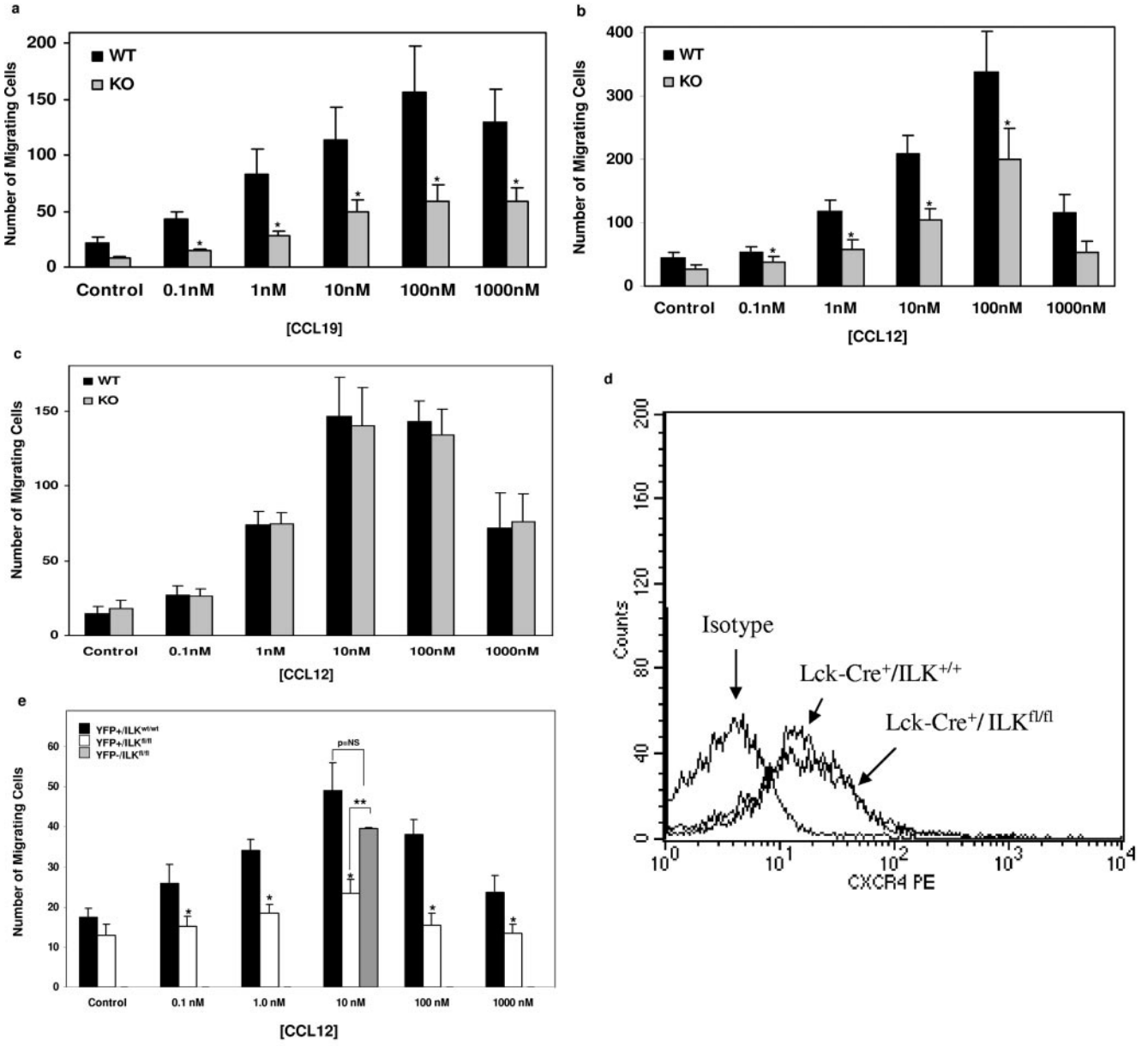

FIG. 4. Abnormal chemotaxis of ILK-deficient T cells. Chemotaxis assays were performed on thymocytes from 3- to 4-week-old mice in transwell chambers to the lymphocyte chemokines (a) CCL19 ($n = 4$, $*P < 0.01$) and (b) CXCL12 ($n = 7$, $*P < 0.01$). (c) CXCL12-triggered chemotaxis of purified lymph node B cells from the same animals ($n = 4$, differences not significant). Cumulative data from the indicated number of experiments are expressed as the means ± standard errors of the means. (d) Representative flow-cytometric analysis of surface $CXCR_4$ expression on T cells. fl/fl, flox/flox. (e) Chemotaxis assays to CXCL12 were performed on flow-sorted lymph node T cells from YFP indicator$^+$ Lck-Cre$^+$/ILK$^{flox/flox}$ and YFP indicator$^+$ Lck-Cre$^+$/ILK$^{WT/WT}$ mice. Cumulative data from three experiments are shown. YFP$^-$ T cells were only studied at 10 nM CXCL12 due to restricted yields. *, $P < 0.01$, compared to YFP indicator$^+$ Lck-Cre$^+$/ILK$^{WT/WT}$ T cells; **, $P < 0.01$ compared to YFP indicator$^+$ Lck-Cre$^+$/ILK$^{flox/flox}$ T cells; p = NS, differences not significant.

relative presence of ILK did not translate into consistent differences in thymic, splenic, or abdominal lymph node architecture between the ILK knockout (KO) mice and littermate controls.

We next explored potential mechanisms related to altered cell trafficking and/or survival that might explain the decreases in thymic cellularity and overall enrichment for ILK competent cells in the spleen and lymph nodes. As previous studies suggested a role for ILK in chemokine-triggered effector functions in leukocytic cell lines (3), we performed chemotaxis assays of T cells in transwell chambers. T cells from the Lck-Cre$^+$/ILK$^{WT/WT}$ littermate mice served as biological controls to rule out theoretical confounders related to Cre expression (13). Lck-Cre$^+$/ILK$^{WT/WT}$ thymocytes from 3- to 4-week-old mice exhibited classic "bell-shaped" results in chemotaxis to the lymphocyte chemokines CXCL12 (stromal cell derived factor [SDF]-1α) and CCL19 (macrophage inflammatory protein [MIP]-3β) (Fig. 4a and 4b). In contrast, chemotaxis of the Lck-Cre$^+$/

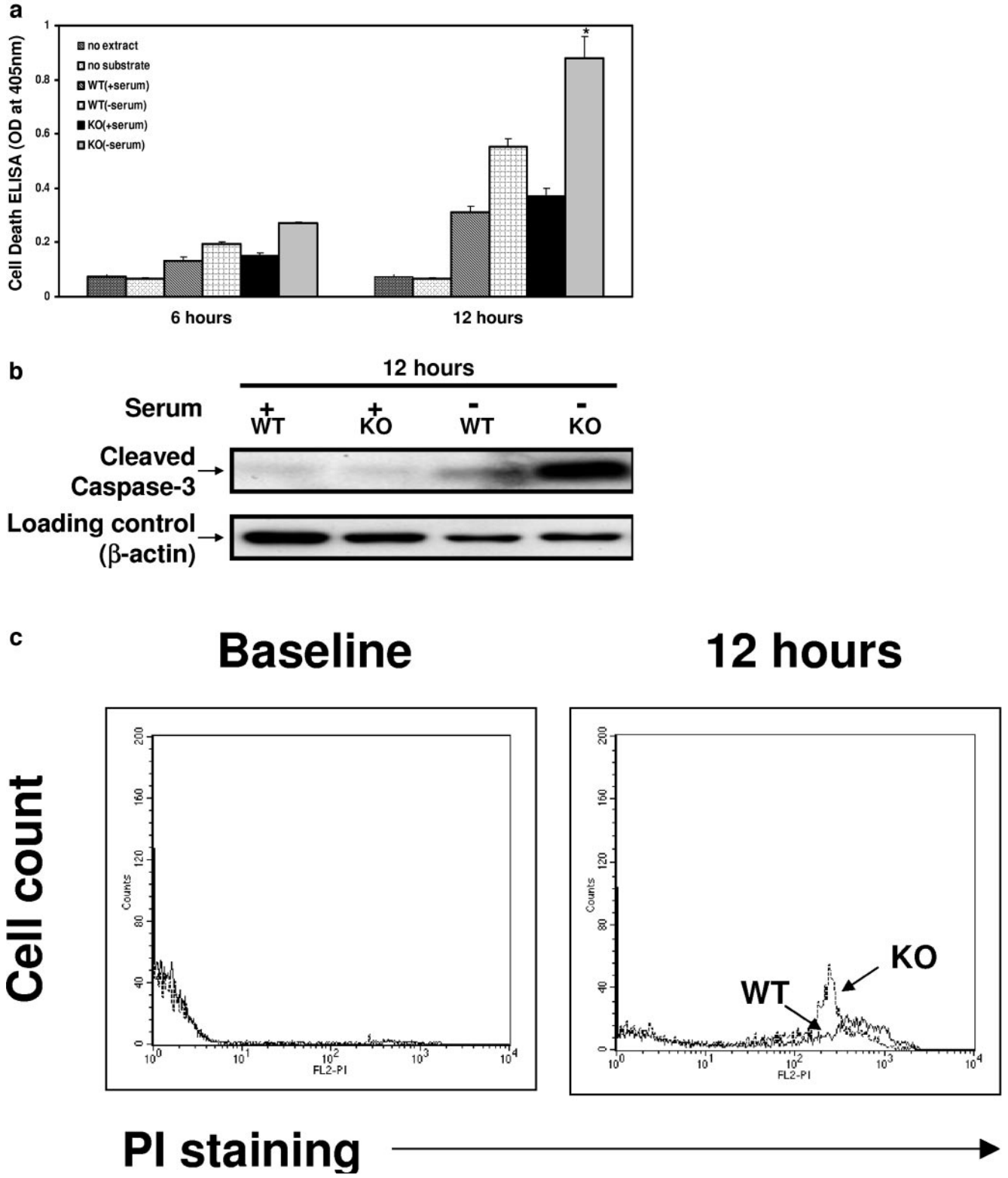

FIG. 5. Diminished survival of ILK KO thymocytes ex vivo. Thymocytes from 3- to 4-week-old mice were isolated and ex vivo cell survival was assessed after 12 h of serum deprivation by (a) cell death detection ELISA ($n = 4$); (b) Western blot analysis probing for cleaved caspase-3; and (c) flow cytometry analysis using propidium iodide. *, $P < 0.03$ compared to WT without serum; OD, optical density.

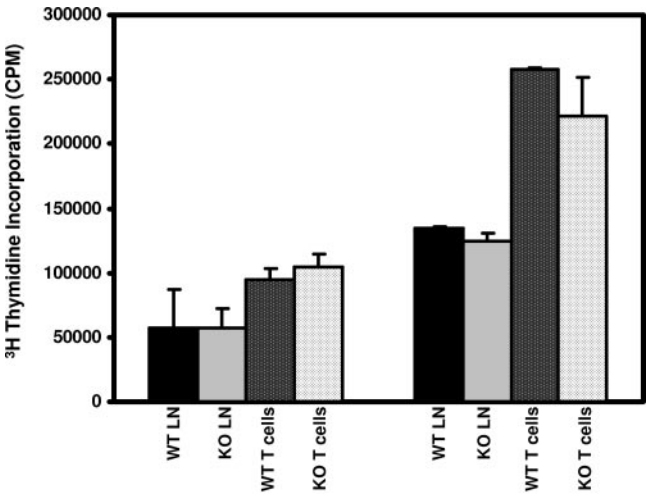

FIG. 6. ILK deletion has no effect on T-cell proliferation. In vitro proliferation assays of lymphocytes were performed using whole lymph nodes or LN T cells purified (91 to 96%) by negative selection column from Lck-Cre$^+$/ILK$^{WT/WT}$ (WT) and Lck-Cre$^+$/ILK$^{flox/flox}$ (KO) mice. Results represent means plus standard errors of the means from four independent experiments done in triplicate assessing [^{3}H]methyl thymidine (10μCi/ml) incorporation following activation of cells (5×10^4 [left] or 1×10^5 [right] cells/well) with plate-bound αCD3 antibody (10 μg/ml 145-2C11; Pharmingen) in 96-well plates for 48 h.

ILK$^{flox/flox}$ T cells, which were indistinguishable from the wild type by flow cytometry analysis, was significantly diminished to both agonists across the broad range of concentrations tested. This defect was T cell-specific, as we saw no difference in chemotaxis of purified lymph node B cells from the same animals (Fig. 4c). It was also not due to modulation of the CXCL12 receptor, $CXCR_4$, on the KO T cells (Fig. 4d). We then repeated the chemotaxis studies using flow-sorted YFP$^+$ lymph node T cells from the triple-transgenic animals, which confirmed the findings observed with the thymocytes (Fig. 4e). Importantly, YFP$^-$ T cells from Lck-Cre$^+$/ILK$^{flox/flox}$ mice, which "escaped" deletion and are ILK competent, demonstrated normal chemotaxis. We saw no effect of ILK deletion on levels of β1-integrins, nor reproducible changes to recombinant vascular cell adhesion molecule (VCAM)-1 in static adhesion assays (not shown).

A growing body of evidence implicates ILK in cell survival pathways (1, 2, 9, 26) that in T cells might account for altered thymic development or result in abnormal stress responses. As noted above, T cells from 3- to 4-week-old ILK-deficient mice were indistinguishable from wild-type T cells as assessed by flow cytometry, including no significant differences in the baseline levels of apoptosis as assessed by PI or annexin V staining (data not shown). We next examined whether stressing these T cells ex vivo might unmask differences between ILK-deficient and ILK-competent cells in susceptibility to apoptosis using three complementary methodologies. We found a significant increase in apoptosis following 12 h of serum deprivation in the isolated ILK KO thymocytes using a cell death ELISA for cytoplasmic histone-associated DNA fragmentation (Fig. 5a). These findings were confirmed by a striking increase in the cleavage product of caspase-3, as assessed by Western blot analysis (Fig. 5b), and a concordant increase in propidium iodide staining in flow cytometry studies (Fig. 5c). Interestingly, in contrast to demonstrated differences in cell survival of Lck-Cre$^+$/ILK$^{flox/flox}$ T cells under stress, we observed no significant differences of in vitro T-cell proliferation upon stimulation with anti-CD3 (Fig. 6) or phorbol-12-myristate-13-acetate–ionomycin (data not shown). Proliferation studies were also performed using YFP$^+$ lymph node T cells from the triple-transgenic animals, and yielded similar results (data not shown).

We next assessed the effects of ILK deletion on intracellular signaling pathways that participate in leukocyte trafficking and survival. In vitro, ILK can serve as a membrane-proximal upstream modulator of Akt, which has been implicated in both pathways (23). The chemokine CXCL12 induced robust Akt activation as assessed by phosphorylation on the activating site, Ser 473 (Fig. 7a), as previously described (29). We observed a reproducible decrease in Ser 473 phosphorylation in ILK-deficient T cells compared to ILK$^{WT/WT}$ cells after 5 min of CXCL12 stimulation. We also performed in vitro assays of Akt activity and found a concordant decrease in Akt kinase function following chemokine stimulation (Fig. 7b).

We finally tested whether ILK deletion modulated the activation of small GTPases such as Rac1 which are important for membrane ruffling and lamellipodia formation as well as chemokine-triggered cell movement (4). In an in vitro kinase assay, we observed significant activation of Rac by the chemokines CXCL12 and CCL19 in T cells isolated from Lck-Cre$^+$/ILK$^{WT/WT}$ mice (Fig. 7c). However, T cells from Lck-Cre$^+$/ILK$^{flox/flox}$ mice showed comparable levels of basal Rac activity though markedly inhibited chemokine-triggered activation. In contrast to the observed abnormalities in Akt and Rac signaling in T cells, kinetic studies showed that chemokine-triggered ERK1/2 phosphorylation was unchanged, thus ruling out global cell signaling changes secondary to ILK deficiency (Fig. 7d).

DISCUSSION

Complete deletion of ILK results in embryonic lethality in every model system so far tested (16, 21, 31). To examine the role of ILK specifically in leukocytes, we generated T cell-specific ILK knockouts by breeding ILK$^{flox/flox}$ mice to transgenic mice expressing Cre recombinase under control of the Lck proximal promoter. While thymic cellularity was comparable in 3- to 4-week-old mice, there was a threefold diminution of thymic T cells by 6 to 8 weeks of age, with the DP population being primarily affected. Analysis of peripheral T cells by quantitative PCR and by breeding Lck-Cre$^+$/ILK$^{flox/flox}$ mice to a YFP-transgenic reporter strain demonstrated an approximate 20-fold enrichment of ILK-competent cells, suggesting these cells have a competitive advantage in trafficking to and/or survival in peripheral lymphatic organs. In exploring potential mechanisms contributing to altered cell survival or trafficking that might contribute to the in vivo findings, we observed a >50% reduction in chemotaxis of ILK-deficient T cells to the chemokines CXCL12 and CCL19. While thymocytes from 3- to 4-week-old ILK KO mice were phenotypically indistinguishable from wild-type thymocytes, including comparable baseline levels of apoptosis, there was enhanced stress-induced apoptosis of ILK-deficient cells upon serum deprivation. Signaling studies in ILK knockout cells

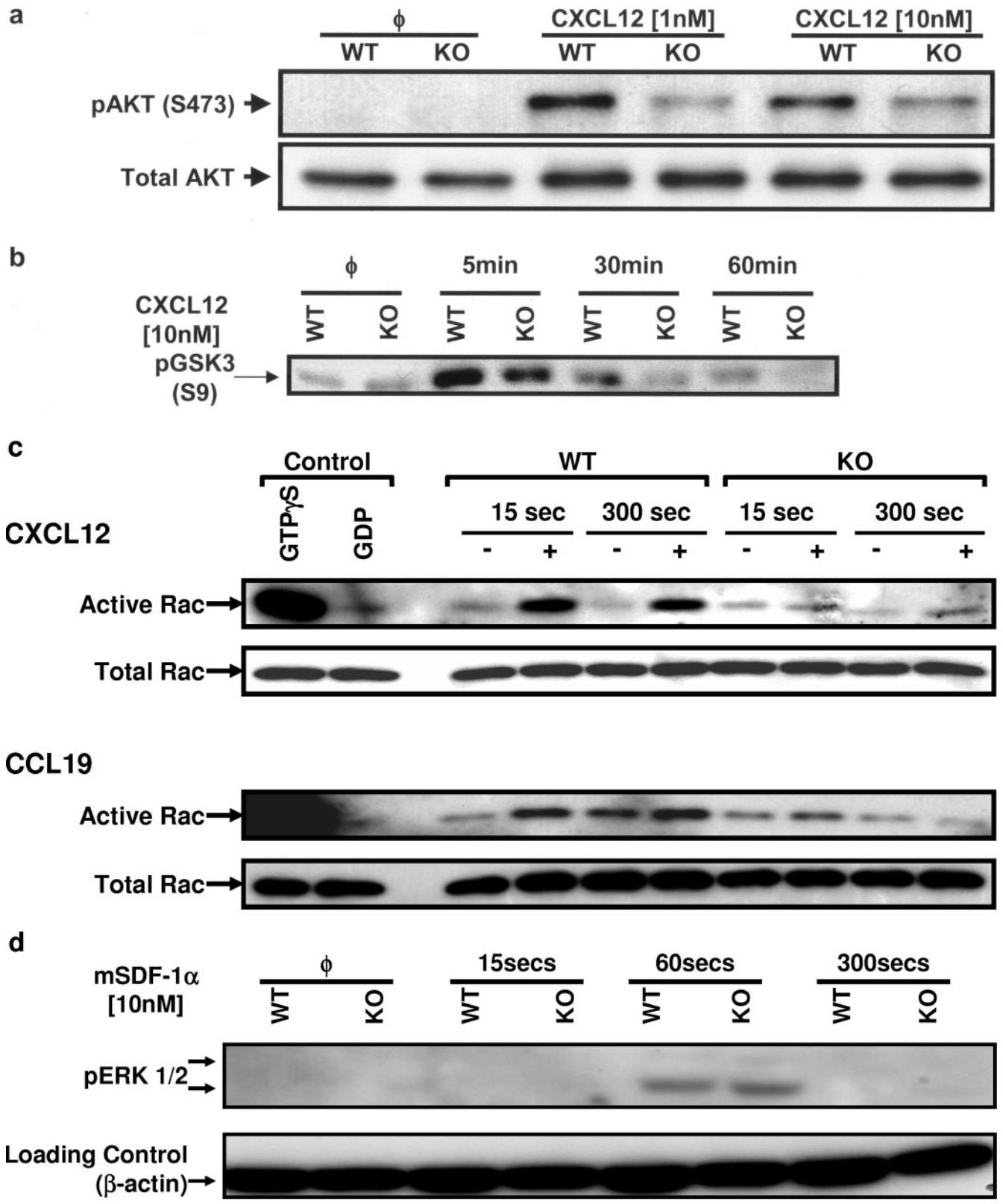

FIG. 7. Effect of ILK deletion on T-cell signaling pathways. Freshly isolated thymic T cells from Lck-Cre^{+}/ILK$^{WT/WT}$ (WT) and Lck-Cre^{+}/ILK$^{flox/flox}$ mice (KO) were incubated with or without CXCL12/CCL19 for the indicated time periods at 37°C. Whole-cell lysates were prepared and assessed as follows: (a) Western blotting for Akt phosphorylation (5 min); (b) kinase activity studies for Akt; (c) kinase activity studies for Rac1; and (d) Western blotting for ERK1/2 phosphorylation. Representative data from one of at least four independent experiments are shown. ϕ, no treatment.

revealed abnormalities in Akt and Rac signaling, two critical pathways in cell movement and survival.

Overexpression of ILK in epithelial cells (10) and a leukocytic cell line (2) have been shown to alter normal cell-matrix interactions. More definitive investigation of endogenous ILK in cell movement has been confounded by the profound effects of complete ILK deletion on survival (21). Two recent studies used the Cre-Lox system to delete ILK specifically in chondrocytes (6, 26), which are not motile cells. The present studies therefore extend prior work, as they clearly indicate a role for ILK in leukocyte chemotaxis to multiple chemokines. As there is still residual chemotactic activity in ILK-deficient T cells, other pathways must contribute to chemotaxis. However, ILK plays a major role in chemotaxis to the chemokines CXCL12 and CCL19 across a wide concentration range.

Perhaps the most striking finding in our signaling studies of ILK-deficient leukocytes was the diminution in Rac activation, which is critical for membrane processes that lead to chemokine-triggered cell movement (4). One other group has recently reported alterations in baseline Rac activation in HeLa cells depleted of ILK and PINCH by siRNA (32). In contrast, our studies show no modulation of basal Rac activity, but severe abrogation of signaling upon chemokine activation. Importantly, we observed these effects as early as 15 seconds following chemokine stimulation. In contrast, abnormalities in Akt signaling occurred only after 5 minutes of chemokine stimulation, as seen in Fig. 7b. Because leukocyte chemotaxis begins within seconds following exposure to chemokines (5), kinetic considerations would suggest that the effects of ILK deletion on Rac signaling are more relevant for chemotaxis, at least immediately following exposure to the stimulus. However, recent chemokine signaling studies have also revealed the importance of longer-acting PTEN-dependent pathways to maintain intracellular gradients of phosphoinositides that in turn reflect persisting extracellular chemoattractant gradients (5). Our studies do not preclude a role for Akt as an ILK-dependent participant in such processes.

Recent studies have elucidated specific ILK binding partners and downstream mediators that modulate actin organization. ILK interacts with α- and β-parvin, which are members of a new family of actin binding proteins shown to be important in the formation of focal adhesion and stress fibers in in vitro systems (18, 32). Via its first ANK domain, ILK may also bind the recently described Pinch 1 and 2 proteins (28), which in turn interact with Nck2, a SH2/SH3-containing adapter protein. It is intriguing to note that α- and β-parvin, Pinch 1, and Nck2 have all been implicated in Rac1 signaling (20, 32). Loss of ILK in fibroblasts and endothelial cells markedly disrupts stress fibers and focal adhesions (2, 21). In contrast to these previous findings, ILK-deficient T cells exhibited no gross abnormalities in cytoskeletal architecture (data not shown). The effects of ILK deletion on the cytoskeleton may be less apparent in nonadherent cells such as leukocytes. However, because differences in Rac signaling occur only upon chemokine stimulation, it is possible that cytoskeletal perturbations become apparent only during active movement.

Our studies are consistent with several recent reports, including work in ILK-deficient endothelial cells (2), which have found a critical role for ILK in apoptosis. In vivo, 6- to 8-week-old ILK-deficient mice have smaller thymuses and a consistent decrease in the double-positive thymocyte population, which is most susceptible to stress-induced cell death in the thymus. A significant increase in apoptotic cells, as revealed by annexin V/PI costaining, was observed in all ILK-deficient thymuses from 6- to 8-week-old mice. Furthermore, seemingly normal thymocytes from 3- to 4-week-old mice had augmented apoptosis upon stress ex vivo. A major finding in two recent descriptions of chondrocyte-specific ILK deletion was the marked reduction of cell proliferation due to alterations in cyclin D1 signaling (6, 27). In contrast, our studies revealed no effects of ILK deletion on T-cell proliferation. While lymphocyte proliferation studies commonly employ anti-αCD3 antibody or calcium ionophores, our work does not preclude a role for ILK in T-cell proliferation to other agonists, though taken together, our findings would likely rule out major effects.

In summary, our genetic studies extend the role of ILK to immune-cell trafficking and survival. These abnormalities become most prominent under conditions that require repetitive cell-matrix interactions or in response to cell stress. These studies have implications for cell recruitment and survival in both homeostatic and pathological processes.

ACKNOWLEDGMENTS

We gratefully acknowledge support from the NIH to T.F. and R.E.G. S.D. is supported by grants from the National Cancer Institute of Canada (NCIC) and the Canadian Institutes for Health Research (CIHR).

REFERENCES

1. **Delcommenne, M., C. Tan, V. Gray, L. Rue, J. Woodgett, and S. Dedhar.** 1998. Phosphoinositide-3-OH kinase-dependent regulation of glycogen synthase kinase 3 and protein kinase B/AKT by the integrin-linked kinase. Proc. Natl. Acad. Sci. USA **95:**11211–11216.
2. **Friedrich, E. B., E. Liu, S. Sinha, S. Cook, D. S. Milstone, C. A. MacRae, M. Mariotti, P. J. Kuhlencordt, T. Force, A. Rosenzweig, R. St.-Arnaud, S. Dedhar, and R. E. Gerszten.** 2004. Integrin-linked kinase regulates endothelial cell survival and vascular development. Mol. Cell. Biol. **24:**8134–8144.
3. **Friedrich, E. B., S. Sinha, L. Li, S. Dedhar, T. Force, A. Rosenzweig, and R. E. Gerszten.** 2002. Role of integrin-linked kinase in leukocyte recruitment. J. Biol. Chem. **277:**16371–16375.
4. **Fukui, Y., O. Hashimoto, T. Sanui, T. Oono, H. Koga, M. Abe, A. Inayoshi, M. Noda, M. Oike, T. Shirai, and T. Sasazuki.** 2001. Haematopoietic cell-specific CDM family protein DOCK2 is essential for lymphocyte migration. Nature **412:**826–831.
5. **Funamoto, S., R. Meili, S. Lee, L. Parry, and R. A. Firtel.** 2002. Spatial and temporal regulation of 3-phosphoinositides by PI 3-kinase and PTEN mediates chemotaxis. Cell **109:**611–623.
6. **Grashoff, C., A. Aszodi, T. Sakai, E. B. Hunziker, and R. Fassler.** 2003. Integrin-linked kinase regulates chondrocyte shape and proliferation. EMBO Rep. **4:**432–438.
7. **Gu, H., J. D. Marth, P. C. Orban, H. Mossmann, and K. Rajewsky.** 1994. Deletion of a DNA polymerase beta gene segment in T cells using cell type-specific gene targeting. Science **265:**103–106.
8. **Gumienny, T. L., E. Brugnera, A. C. Tosello-Trampont, J. M. Kinchen, L. B. Haney, K. Nishiwaki, S. F. Walk, M. E. Nemergut, I. G. Macara, R. Francis, T. Schedl, Y. Qin, L. Van Aelst, M. O. Hengartner, and K. S. Ravichandran.** 2001. CED-12/ELMO, a novel member of the CrkII/Dock180/Rac pathway, is required for phagocytosis and cell migration. Cell **107:**27–41.
9. **Hannigan, G., A. A. Troussard, and S. Dedhar.** 2004. Integrin linked kinase: A cancer therapeutic target unique among its ILK. Nat. Rev. Cancer **5:**51–63.
10. **Hannigan, G. E., C. Leung-Hagesteijn, L. Fitz-Gibbon, M. G. Coppolino, G. Radeva, J. Filmus, J. C. Bell, and S. Dedhar.** 1996. Regulation of cell adhesion and anchorage-dependent growth by a new beta 1-integrin-linked protein kinase. Nature **379:**91–96.
11. **Hirsch, E., V. L. Katanaev, C. Garlanda, O. Azzolino, L. Pirola, L. Silengo, S. Sozzani, A. Mantovani, F. Altruda, and M. P. Wymann.** 2000. Central role for G protein-coupled phosphoinositide 3-kinase gamma in inflammation. Science **287:**1049–1053.
12. **Lee, P. P., D. R. Fitzpatrick, C. Beard, H. K. Jessup, S. Lehar, K. W. Makar, M. Perez-Melgosa, M. T. Sweetser, M. S. Schlissel, S. Nguyen, S. R. Cherry, J. H. Tsai, S. M. Tucker, W. M. Weaver, A. Kelso, R. Jaenisch, and C. B.**

Wilson. 2001. A critical role for Dnmt1 and DNA methylation in T cell development, function, and survival. Immunity **15:**763–774.
13. **Lewandoski, M.** 2001. Conditional control of gene expression in the mouse. Nat. Rev. Genet. **2:**743–755.
14. **Li, Z., H. Jiang, W. Xie, Z. Zhang, A. V. Smrcka, and D. Wu.** 2000. Roles of PLC-beta2 and -beta3 and PI3Kgamma in chemoattractant-mediated signal transduction. Science **287:**1046–1049.
15. **Luster, A. D.** 1998. Chemokines—chemotactic cytokines that mediate inflammation. N. Engl. J. Med. **338:**436–445.
16. **Mackinnon, A. C., H. Qadota, K. R. Norman, D. G. Moerman, and B. D. Williams.** 2002. C. elegans PAT-4/ILK functions as an adaptor protein within integrin adhesion complexes. Curr. Biol. **12:**787–797.
17. **Matsui, T., L. Li, F. del Monte, Y. Fukui, T. Franke, R. Hajjar, and A. Rosenzweig.** 1999. Adenoviral gene transfer of activated PI 3-kinase and Akt inhibits apoptosis of hypoxic cardiomyocytes in vitro. Circulation **100:**2373–2379.
18. **Nikolopoulos, S. N., and C. E. Turner.** 2000. Actopaxin, a new focal adhesion protein that binds paxillin LD motifs and actin and regulates cell adhesion. J. Cell Biol. **151:**1435–1448.
19. **Peirson, S. N., J. N. Butler, and R. G. Foster.** 2003. Experimental validation of novel and conventional approaches to quantitative real-time PCR data analysis. Nucleic Acids Res. **31:**e73.
20. **Rosenberger, G., I. Jantke, A. Gal, and K. Kutsche.** 2003. Interaction of alphaPIX (ARHGEF6) with beta-parvin (PARVB) suggests an involvement of alphaPIX in integrin-mediated signaling. Hum. Mol. Genet. **12:**155–167.
21. **Sakai, T., S. Li, D. Docheva, C. Grashoff, K. Sakai, G. Kostka, A. Braun, A. Pfeifer, P. D. Yurchenco, and R. Fassler.** 2003. Integrin-linked kinase (ILK) is required for polarizing the epiblast, cell adhesion, and controlling actin accumulation. Genes Dev. **17:**926–940.
22. **Sasaki, T., J. Irie-Sasaki, R. G. Jones, A. J. Oliveira-dos-Santos, W. L. Stanford, B. Bolon, A. Wakeham, A. Itie, D. Bouchard, I. Kozieradzki, N. Joza, T. W. Mak, P. S. Ohashi, A. Suzuki, and J. M. Penninger.** 2000. Function of PI3Kgamma in thymocyte development, T cell activation, and neutrophil migration. Science **287:**1040–1046.
23. **Servant, G., O. D. Weiner, P. Herzmark, T. Balla, J. W. Sedat, and H. R. Bourne.** 2000. Polarization of chemoattractant receptor signaling during neutrophil chemotaxis. Science **287:**1037–1040.
24. **Srinivas, S., T. Watanabe, C. S. Lin, C. M. William, Y. Tanabe, T. M. Jessell, and F. Costantini.** 2001. Cre reporter strains produced by targeted insertion of EYFP and ECFP into the ROSA26 locus. BMC Dev. Biol. **1:**4.
25. **Takesono, A., R. Horai, M. Mandai, D. Dombroski, and P. L. Schwartzberg.** 2004. Requirement for Tec kinases in chemokine-induced migration and activation of Cdc42 and Rac. Curr. Biol. **14:**917–922.
26. **Terpstra, L., J. Prud'homme, A. Arabian, S. Takeda, G. Karsenty, S. Dedhar, and R. St.-Arnaud.** 2003. Reduced chondrocyte proliferation and chondrodysplasia in mice lacking the integrin-linked kinase in chondrocytes. J. Cell Biol. **162:**139–148.
27. **Troussard, A. A., N. M. Mawji, C. Ong, A. Mui, R. St.-Arnaud, and S. Dedhar.** 2003. Conditional knock-out of integrin-linked kinase demonstrates an essential role in protein kinase B/Akt activation. J. Biol. Chem. **278:**22374–22378.
28. **Tu, Y., F. Li, S. Goicoechea, and C. Wu.** 1999. The LIM-only protein PINCH directly interacts with integrin-linked kinase and is recruited to integrin-rich sites in spreading cells. Mol. Cell. Biol. **19:**2425–2434.
29. **Turner, L., S. G. Ward, and J. Westwick.** 1995. RANTES-activated human T lymphocytes. A role for phosphoinositide 3-kinase. J. Immunol. **155:**2437–2444.
30. **Wu, C.** 1999. Integrin-linked kinase and PINCH: partners in regulation of cell-extracellular matrix interaction and signal transduction. J. Cell Sci. **112:**4485–4489.
31. **Zervas, C. G., S. L. Gregory, and N. H. Brown.** 2001. Drosophila integrin-linked kinase is required at sites of integrin adhesion to link the cytoskeleton to the plasma membrane. J. Cell Biol. **152:**1007–1018.
32. **Zhang, Y., K. Chen, Y. Tu, and C. Wu.** 2004. Distinct roles of two structurally closely related focal adhesion proteins, alpha-parvins and beta-parvins, in regulation of cell morphology and survival. J. Biol. Chem. **279:**41695–41705.